ESP IJAST
ESP International Journal of Advancements in Science & Technology
ISSN: 2583-9233 / Volume 2 Issue 1 March 2024 / Page No: 52–59
Paper Id: IJAST-V2I1P108 / Doi: 10.56472/25839233/IJAST-V2I1P108

Original Article

Green Synthesis, Characterization and Corrosion Studies of Mild Steel by Using Novel Inhibitor of *Acalypha Wilkesiana*

Sunitha K[1], Swamy M T[2], Pruthviraj R D[3]
[1,2]*Chemistry R & D Centre, Department of Chemistry, Sambhram Institute of Technology, Bangalore, India.*
[3]*Chemistry R & D Centre, Department of Chemistry, Rajarajeswari College of Engineering, Bangalore, India.*

Received Date: 30 December 2023 Revised Date: 24 January 2024 Accepted Date: 06 March 2024

Abstract: *Lemon juice extract was used in the solution combustion method to create the acalypha wilkesiana. For mild steel, the artificial acalypha wilkesiana showed corrosion inhibition. The surface characteristics of surfaces treated with inhibitors and untreated surfaces are analysed using the resulting sem and tem micrographs. It demonstrates that, in comparison to free mild steel, the stressed surface of Acalypha Wilkesiana has a greater potential to avoid corrosion. The potentiodynamic values showed that mild steel with varying concentrations had a greater propensity to resist corrosion in a 1 m hydrochloric acid solution at temperatures of 250 and 350 degrees Celsius. Tafel polarisation and electrochemical impedance were examined at various concentrations at 250 and 350 degrees Celsius. the rate of adsorption rises as the concentrations of the inhibitors do.*

Keywords: *Mild Steel,* Acalypha Wilkesiana *Inhibitor, Weight Loss Measurement, Potentiometric Polarization, Scanning Electron Microscope, TEM, Tafel Polarization, EDAX.*

I. INTRODUCTION

Growing interest has been shown recently in the use of green chemistry to synthesise biocompatible metal nanoparticles (NPs) and their potential uses in biomedicine (Zhang et al., 2016). Modern advances in science and industry are gradually being combined with "Green Chemistry" and chemical processes as part of global efforts to reduce created hazardous waste. This study's "green" synthesis of silver nanoparticles used a wet chemistry process in a single pot to synthesise therapeutic plant extract using a bottom-up strategy. According to Shiv et al. (2003) and Yong and Kim (2008), this method produces stable, evenly distributed silver nanoparticles with minimal aggregation and good size control. It is also inexpensive and environmentally safe. In this investigation, an extract from Acalypha wilkesiana was utilised as a stabilising and reducing agent. Often known as Irish petticoat, this plant is indigenous to the South Pacific islands and is a member of the Euphorbiaceae family.

Plants such as Acalypha wilkesiana are often found at Landmark University in Nigeria, West Africa. Its therapeutic benefits have been established. This plant, sometimes known as Jacob's coat or copperleaf, grows well in both partial shade and full sun. The broad, big leaves have teeth along the edges and might be flat or wrinkled. It measures roughly 2-3 metres in height, 10-15 centimetres in length, and 15 centimetres in width. Because of its eye-catching red colouring, it is a commonly grown outdoor decorative plant. It is prized for its extensive array of hedging and variegated cultivars (Nagarajan et al., 2003). Millions of people continue to use naturally occurring, inexpensive, and environmentally safe therapeutic plants like Acalypha wilkesiana despite advancements in medical research. The therapeutic properties of A. wilkesiana extend to both its leaves and seeds. It has been used to treat a variety of illnesses in poor nations. Its efficacy in treating malaria, skin conditions, gastrointestinal issues, hypertension, diabetes mellitus, and breast tumours has been documented by researchers in Western Nigeria (Udobang et al., 2010; Akinyemi et al., 2006; Oyelani et al., 2003)..

A innovative technique that has attracted the attention of multiple researchers is the use of plant extract as a stabilising and reducing agent in the green manufacture of silver nanoparticles. Using geranium leaf aqueous extract as a reducing agent, Rivera-Rangel et al. (2018) worked on the green synthesis of silver nanoparticles in oil-in-water microemulsion and nano-emulsion. Silver nanoparticles (AgNPs) were synthesised by Ajayi and Afolayan (2016) using an alkalinized leaf extract of Cymbopogon citrates. Umadevi et al. (2012) conducted a study on the biosynthesis of silver nanoparticles (NPs) using Dillenium carota extract. The study examined the effects of different doses of D. carota extract. In order to achieve a straightforward and economical bio-reduction of silver nanoparticles utilising Terminalia arjuna plant extract, Ahmed and Ikram (2015) employed the one-pot green synthesis approach. Kaumeel, investigated the demonstration of a viable method for the biogenic manufacture of

 This is an open access article under the CC BY-NC-ND license (https://creativecommons.org/licenses/by-nc-nd/2.0/)

silver nanoparticles using the leftover biomass from the lipid extraction of Acutodesmus dimorphus microalgae grown in dairy effluent. In 2016, Shankar et al. used algae to biosynthesize gold and silver nanoparticles. In our earlier research, we synthesised silver nanoparticles using extracts from the plants Calotropis procera and Tithonia diversifolia (Dada et al., 2016, 2018b). The following is an additional list of works on the environmentally friendly synthesis of silver nanoparticles utilising various plant extracts: (Vijayaraghavan et al., 2012); Thevetia peruviana Juss (Oluwaniyi et al., 2015); banana peel extract (Ibrahim, 2015); Acalypha indica leaf extract (Krishnaraj et al., 2010); Punica granatum peel extract (Edison & Sethuraman, 2013); Calotropis procera extract (Dada et al., 2017b).

In order to determine the lowest concentration at which nanoparticle growth is feasible, this study examined a number of operational factors, including the effect of concentration and volume ratio. Despite the extensive research conducted, the factors influencing the synthesis of silver nanoparticles have not been fully taken into account when it comes to the experimental optimisation of operational parameters. Thus, the need for this study stems from the lack of previous reports on the phytochemical screening of Acalypha wilkesiana leaf extract, experimental parameter optimisation crucial to the green synthesis of Acalypha wilkesiana silver nanoparticles (AW-AgNPs), and the characterization and application of AW-AgNPs on Multi-Drug Resistance Micro-organisms.

II. EXPERIMENTAL

A. Materials and Methods

Nigeria's Acalypha wilkesiana (AW) plant (Fig. 1) was gathered close to Landmark University. It was then cleansed to get rid of the dirt from the farm and allowed to air dry to preserve the essential volatile molecules. As in our earlier research, the process for extract preparation and AW-AgNP synthesis was followed (Dada et al., 2017b, 2018b). Typically, the process involved measuring out 10 mL of the leaf extract, pouring it into a clean 250 mL beaker, and allowing it to react with 90 mL of room temperature 1 × 10−3 M AgNO3. On the mechanical shaker, the resultant solution was agitated under ideal operating circumstances The silver nanoparticles (AW-AgNPs) derived from Acalypha wilkesiana were separated by centrifugation at 4000 rpm during the ideal contact time. To find out if the AW leaf extract included any phenols, saponins, triterpenes, flavonoids, alkaloids, or steroids, phytochemical screening was done. These several tests were conducted in accordance with the methodology described in the literature (Senguttuvan et al., 2014) and in our prior study (Dada et al., 2018b). Using a combination of spectroscopic techniques, including Fourier Transform Infrared (FTIR), Scanning Electron Microscopy (SEM) in conjunction with Energy Dispersive X-ray (EDX), Transmission Electron Microscopy (TEM), and Ultraviolet Visible (UV-Vis) spectroscopy, the synthesised AW-AgNPs were characterised.

Figure 1: Acalypha Wilkesiana (AW) Plant

III. RESULTS AND DISCUSSION

A. Characterization of ***Acalypha wilkesiana***

a) XRD Analysis

The powder XRD pattern of Acalypha wilkesiana, which was created using the thermal breakdown method, is shown in Figure 1. All of the XRD peaks have lattice parameter values of a = 5.1956 Å, b = 5.0935 Å, and c = 11.7045 Å, and may be easily indexed to monoclinic Acalypha wilkesiana. The lack of peaks found as a result of impurity phases suggests that the product is extremely pure. The narrowness of the diffraction peaks was noted. Using the Scherrer formula, the average crystallite size of the $BiVO_4$ nanoparticles was determined to be 39 nm[1].

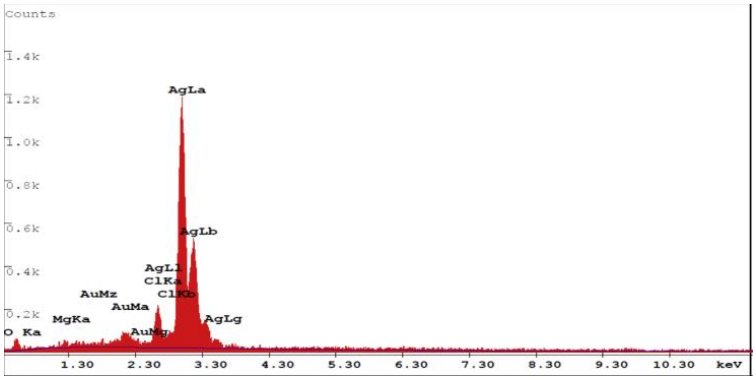

Figure 2: XRD pattern of Acalypha wilkesiana

b) FTIR Analysis

The unshared V=O stretching vibrations are responsible for the band observed at 1,021 cm−1. Two vanadium atoms (V–O–V) share antisymmetric stretching vibrations of the bonded oxygen, which give rise to the bands at 833 and 706 cm−1, while the symmetric stretching mode of V–O–V units is represented by a band at 615 cm−1. Furthermore, the O-H stretching and bending vibration of lattice water molecules is responsible for the bands that are present at 3,402 and 1,627 cm−1.

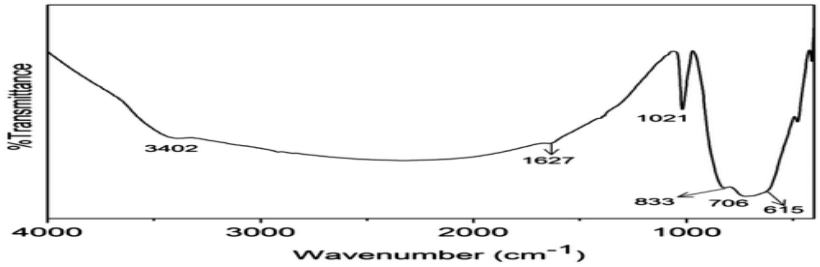

Figure 3: FTIR Analysis of Acalypha wilkesiana

c) Morphology, Microstructure and Elemental Analysis

Using TEM and FESEM, the surface morphology of artificial Acalypha wilkesiana was examined.The FE-SEM results unmistakably demonstrate the spherical shape of the synthesised Acalypha wilkesiana, which was created using an aqueous leaf extract of Ficus hispida. Representative FESEM photos of this product were shown. The effective synthesis of Acalypha wilkesiana and its capping by photoconstituents found in plant extract are both confirmed by the presence of elemental Ag, C, and O. showed TEM pictures of Acalypha wilkesiana that had been produced using an aqueous leaf extract of Ficus hispida Linn. f. Acalypha wilkesiana has a spherical shape with an average particle size of 20 nm, according to TEM data. The polycrystalline nature of Acalypha wilkesiana is suggested by the ring-like diffraction pattern shown in the selected area electron diffraction (SAED) patterns, which are in excellent accord with earlier research. The same apparatus was used for the EDAX measurements, and the SEM images provided morphological information on the MILD STEEL surface both before and after corrosion in the acidic media, as well as surface morphology of the inhibited surface.

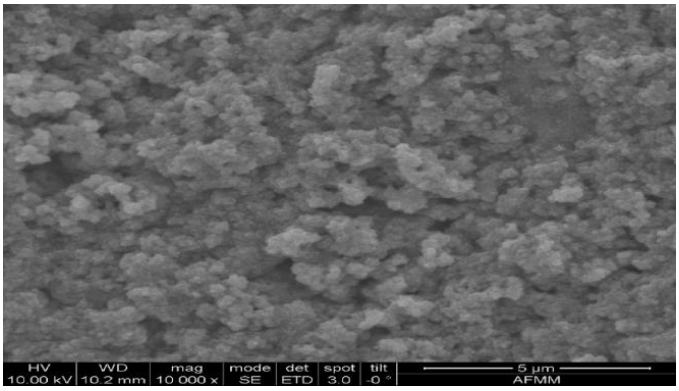

Figure 4: SEM images of Aluminium Alloy (A) In the Absence Acalypha wilkesiana

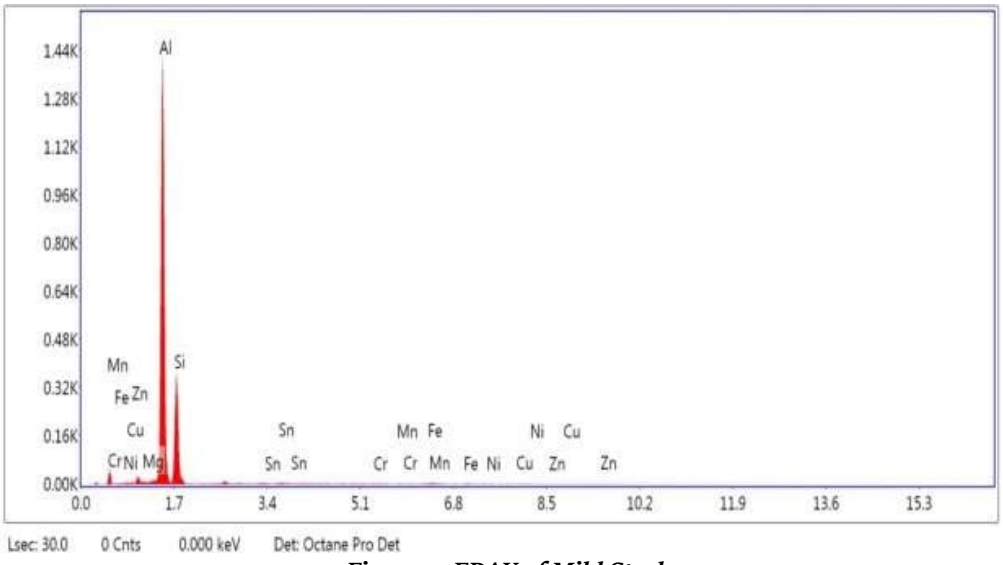

Figure 5: EDAX of Mild Steel

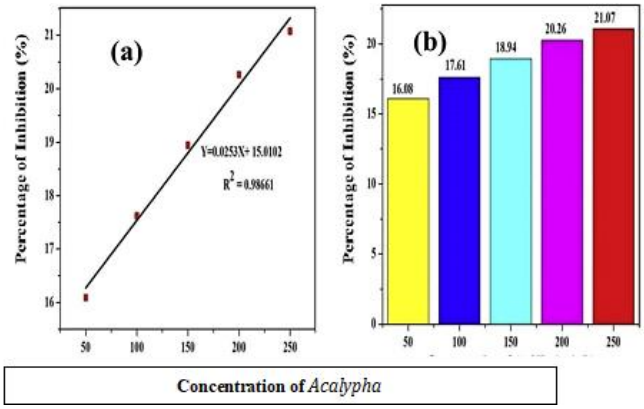

Figure 6: Concentration of Acalypha

B. Weight Loss Measurements

For a whole day at 250°C and 350°C, the 2.5 cm, 2 cm, and 0.025 cm Al-2014 alloy that had been treated with an inhibitor and the untreated alloy were stored in 250 cc of 1.0 M HCl. Acetone and deionized water are used to cleanse the surface when it is colder than room temperature. In an acidic solution, the Al-2014 alloy's surface causes weight to decrease. Gravimetric analysis provided an accurate measurement of the weight loss orders (99.8%). The relationship (1) has been used to estimate the corrosion penetration rate (CPR).18–20 The relationship (2) was used to calculate the inhibitory efficiency.

C. Analysis of Electrochemistry Tafel Polarization Studies

The ASTM G3-73 standard is used for the electrochemical investigations, and CH-INSTRUMENT (USA) is used.21 To ensure uniformity in the range of -250 to +250 mV, the working terminal is dipped in the electrolyte solution for 30 minutes. The potential rate of 0.166 mV sec-1 represents the polarisation rate.

D. Electrochemical Impedance Spectroscopy

EIS was conducted in the acidic medium for all mild steel samples with and without inhibitorsby applying AC signals with a10-mV amplitude and 1.0 M Hertz–10.0MHertz frequency range.[22]

E. Microstructural and Elemental Analysis

The mild steel samples in 1.0 molar hydrochloric acid solution are shown in Figure 2 both with and without the proper doses of inhibitor 3a (A–D). The results indicate that the presence of the inhibitor significantly reduced the corrosion on the mild steel surface. Furthermore, we found that, in contrast to the inhibitor-treated surface, the pits and cavities on the inhibitor-untreated surface were not as visible. However, pits and cracks were visible in the inhibited surface at a concentration of 50 ppm.

This indicates that localised material erosion occurs when there are no inhibitors in the acidic environment. Pits and erosion are still evident when employing a 50 ppm inhibitor, but they are less so than previously. Pits and erosion continue to decrease with concentrations between 50 and 100 ppm; pits and erosion were reduced at concentrations of 150 ppm.

F. Weight Loss Studies

At 250 and 350 degrees Celsius, the inhibitory efficiency (ηWL%) and corrosion penetration rate of inhibitor 3a aniline in 1 molar hydrochloric acid were evaluated and estimated for mild steel. The results are summarised in Table 2. When the concentration of the inhibitor Acalypha wilkesiana was raised, the corrosion efficiency dropped. The rate of corrosion on the untreated surface is high. A similar trend is seen in the treated surface's low rate of corrosion at 250°C and 350°C. 23–24 In the 1.0 molar hydrochloric acid solution, Acalypha wilkesiana has a stronger inhibitory potency, and corrosion occurs more quickly at 350 degrees Celsius than it does at 250 degrees.

G. Tafel Polarization Measurement

Figure-4 demonstrates the Tafel polarisation at 250 and 350 degrees Celsius. The calculated results are shown in Table 3. Following the addition of Acalypha wilkesiana iron steel, a decrease in current density was seen in the polarisation curve fluctuation. While Icorr values gradually decreased, the efficiency of corrosion rose with inhibitor concentrations, suggesting that the inhibitor-established protective coating covered the mild steel surface. When compared to the unreacted (blank), the corrosion inhibitors had a significant effect on the Ecorr values for the synthesised chemical. Acalypha wilkesiana Sat, at a concentration of 150 ppm, has the biggest Ecorr displacement (0.674 mV). The cathodic/anodic slant Tafel lines are not sporadically shifted by altering inhibitor fixations, which are also conveyed. The steady values of the $'\beta c'$ and $'\beta'$ are generally exclusive to blank, untreated samples. The mild steel will then develop coatings from Acalypha wilkesiana, which will prevent the rusting. 25 The rates at which corrosion penetrated were decreased. Using the accompanying relations, we were able to determine the erosion effectiveness from the plots (3).

$$\eta\text{Tafel \%} = I_{corr} / (1 - 0) \times 100 \qquad (3)$$

Where I_{corr} Current density with Corrosion inhibitor; I_{corr} Density without corrosion inhibitor

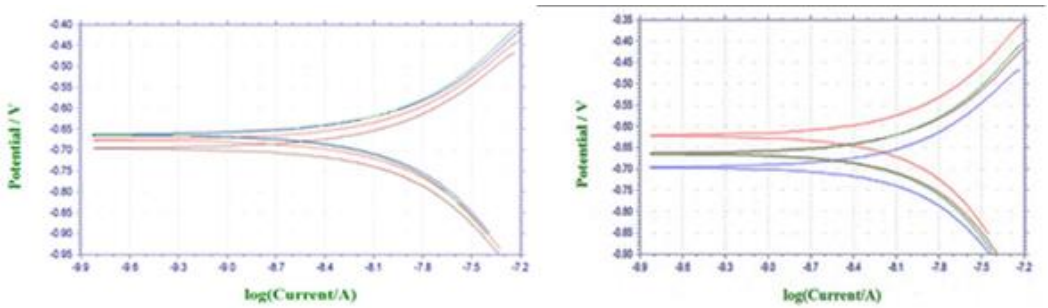

Figure 7: Tafel Polarization Curves at a) 25°C and b) 35°C by using Acalypha Wilkesiana Inhibitor

H. Electrochemical Impedance Studies

Strange conclusions could need to be drawn after carefully examining certain data, such as the following: The improvement of any Acalypha wilkesiana reinforcement is followed by an advancement towards lower decreasing perspective thickness for each anodic and cathodic Tafel polarisation turn. When Icorr respects decline, it suggests that a protective film is forming at the Al 2014 surface.

The vicinity of the breaking down inhibitors shifts Ecorr values elegantly when compared to the uninhibited bend (clear). The most significant development of Ecorr main set at respect for 100ppm is 24.2 milli Volts, which is much less than the 85.1 milli Volts.26 The dislodging cutoff is greater than 85 mV, if nothing else.27–28 Therefore, in order to lessen the crumbling charges after completion, the four Acalypha wilkesiana subordinates are the mix type utilisation inhibitor with the guidance of techniques for barricading structure on easily accessible mild steel flamboyant spots. The fact that they aren't trading is promising.

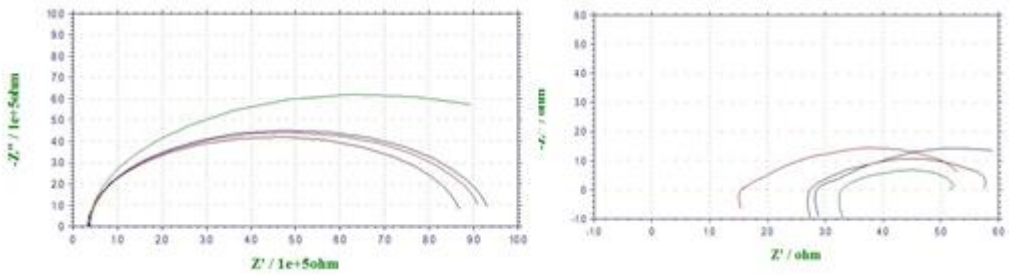

Figure 5: EIS Curves at a) 25°C and b) 35°C by using Acalypha wilkesiana

I. Adsorption Isotherm

The rate of inhibition that is directly impacted by the adsorbent on the metal surface was predicted using the adsorption isotherm equation.29–30 Inhibition of adsorption was investigated based on the factor (Kads).

IV. CONCLUSION

The mild steel microstructure analysis at 150 ppm shows that it has less of a tendency to corrode. It also verified that, when utilising the weight loss method, the percentage of inhibitory efficiency, or ηWL%, is approximately 44.04 percent (at 250C) and 48.51 percent (at 350C). It was decided to use the Tafel polarisation system. The information gathered leads to the following conclusions: Mix-type inhibitors decrease Al-2014 corrosion in 1.0 M HCl more effectively as inhibitor concentrations rise.

Table 1: Weight% of Elements in the Aluminium 2014

Elements	Mg	Sn	Cr	Mn	Fe	Ni	Si	Cu	Zn	Al
(Wt. %)	0.22	0.34	0.11	0.16	0.74	0.35	0.8	0.4	0.2	Balance

Table 2: Inhibitor Concentration (C), Corrosion Penetration Rate (CPR) and Inhibition Efficiency for mild steel in the Acidic Medium (1M HCl)

Temperature(°C)	Concentration(ppm)	Corrosion rate(mpy)	% Efficiency (ηWL %)
25	Blank	3.235	-
	50	2.735	15.41%
	100	2.223	31.28%
	150	1.810	44.04%
35	Blank	3.968	-
	50	3.316	16.43%
	100	2.696	32.05%
	150	2.043	48.51%

Table 3: Tafel Polarization Parameters at Different Concentrations

Temperature	Concentration (ppm)	Icorr	Ecorr	βC	βa	Ŋ % Tafel	Surface coverage (θ)
25°C	Blank	1956	-0.712	106.2	54.2	-----	----
	50	1365	-0.682	110.7	54.7	30.21%	0.302
	100	674	-0.661	107.9	53.6	65.54%	0.655
	150	463	-0.642	109.5	54.2	76.32%	0.763
35°C	Blank	2578	-0.674	119.4	53.1	----	----
	50	1437	-0.672	125.2	54.3	44.25%	0.442
	100	1002	-0.669	128.5	54.8	61.13%	0.611
	150	837	-0.647	121.4	56.2	67.53%	0.675

Table 4: Kads and (ΔG^o)

Temperature (^oC)	Concentration (ppm)	Concentration (m-mole)	Θ	*K*ads (KJ per mol)	ΔGo (KJ per mol)
25^{o}C	Blank	-	-	-	-
	50	0.3141	0.302	1377.00	-27.857
	100	0.6282	0.655	3022.20	-29.805
	150	0.9423	0.763	3416.54	-30.109
35^{o}C	Blank	-	-	-	-
	50	0.13684	0.442	2521.85	-30.342
	100	0.27370	0.611	2500.30	-30.320
	150	0.41050	0.675	2204.00	-29.999

V. REFERENCES

[1] Ahmed S., Ikram S. Synthesis of gold nanoparticles using plant extract: an overview. *Nano Res. Appl.* 2015;1(1):1–6. http://nanotechnology.imedpub.com/archive.php [Google Scholar]

[2] Ajayi E., Afolayan A. Green synthesis, characterization and biological activities of silver nanoparticles from alkalinized *Cymbopogon citratus Stapf*. *Adv. Nat. Sci. Nanosci. Nanotechnol.* 2017;8(1):015017. [Google Scholar]

[3] Akinyemi K.O., Olukayode O.C., Fasure O. Screening of crude extracts of six medicinal plants used in South-west Nigerian unorthodox medicine for anti-methicillin resistant Staphylococcus aureus activity. *BMC Complement Altern. Med.* 2006:1–7. [PMC free article] [PubMed] [Google Scholar]

[4] Babu S.A., Prabu H.G. Synthesis of AgNPs using the extract of Calotropis procera flower at room temperature. *Mater. Lett.* 2011;65(11):1675–1677. [Google Scholar]

[5] Bindhu M.R., Umadevi M. Silver and gold nanoparticles sensor and antibacterial applica-02 tions. *Spectrochim. Acta Part A Molecular and Biomolecular Spectroscopy.* 2014;2014(128):37–45. [PubMed] [Google Scholar]

[6] Dada A.O., Adekola F.A., Odebunmi E.O. Kinetics and equilibrium models for sorption of Cu(II) onto a novel manganese nano-adsorbent. *J. Dispersion Sci. Technol.* 2016;37(1):119–133. [Google Scholar]

[7] Dada A.O., Adekola F.A., Odebunmi E.O. Liquid phase scavenging of Cd (II) and Cu (II) ions onto novel nanoscale zerovalent manganese (nZVMn): equilibrium, kinetic and thermodynamic studies. *Environ. Nanotechnol. Monit. Manag.* 2017;8:63–72. [Google Scholar]

[8] Dada A.O., Ojediran O.J., Dada F.E., Olalekan A.P., Awakan O.J. Green synthesis and characterization of silver nanoparticles using *Calotropis procera* extract. *J. Appl. Chem. Sci. Int.* 2017;8(4):137–143. [Google Scholar]

[9] Dada A.O., Adekola F.A., Odebunmi E.O. Kinetics, mechanism, isotherm and thermodynamic studies of liquid phase Adsorption of Pb^{2+} onto wood activated carbon supported zerovalent iron (WAC-ZVI) nanocomposite. *Cogent Chem. J.* 2017;3 1351653, pg 1- 20. [Google Scholar]

[10] Dada A.O., Adekola F.A., Adeyemi O.S., Bello M.O., Adetunji C.O., Awakan O.J. 2018. Silver Nanoparticles - Fabrication, Characterization and applications; pp. 165–184. Chapter 9. [Google Scholar]

[11] Dada A.O., Inyinbor A.A., Idu I.E., Bello O.M., Oluyori A.P., Adelani –Akande T.A., Okunola A.A., Dada O. Eff ect of operat ional param eters, charact erization and anti-bacterial studies of green synthesis of Silver Nano particles, using *Tithonia diversifolia*. *PeerJ.* 2018;6 [PMC free article] [PubMed] [Google Scholar]

[12] Davidović S., Lazić V., Vukoje I., Papan J., Anhrenkiel S.P., Dimitrijević S., Nedeljković J.M. Dextran coated silver nanoparticles — chemical sensor for selective cysteine detection. *Colloids Surfaces B Biointerfaces.* 2017;160(2017):184–191. [PubMed] [Google Scholar]

[13] Edison T.J.I., Sethuraman M.G. Biogenic robust synthesis of silver nanoparticles using Punica granatum peel and its application as a green catalyst for the reduction of an anthropogenic pollutant 4-nitrophenol. *Spectrochim. Acta A Mol. Biomol. Spectrosc.* 2013;104:262–264. [PubMed] [Google Scholar]

[14] Femi-Adepoju A.G., Dada A.O., Otun K.O., Adepoju A.O., Fatoba O.P. Green synthesis of silver nanoparticles using terrestrial fern (*Gleichenia Pectinata* (Willd.) C. Presl.): characterization and antimicrobial studies. *Heliyon.* 2019;5(2019) [PMC free article] [PubMed] [Google Scholar]

[15] Ibrahim H.M.M. Green synthesis and characterization of silver nanoparticles using banana peel extract and their antimicrobial activity against representative microorganisms. *J. Radiat. Res. Appl. Sci.* 2015;8:265–275. [Google Scholar]

[16] Jyoti M., Baunthiyal M., Singh A. Characterization of silver nanoparticles synthesized using Urticadioica Linn. leaves and their synergistic effects with antibiotics. *J. Radiat. Res. Appl. Sci.* 2016;9:217–227. [Google Scholar]

[17] Kaumeel C., Imran P., Tonmoy G., Chetan P., Rahulkumar M., Arup G., Sandhya M. Green synthesis, characterization and antioxidant potential of silver nanoparticles biosynthesized from de-oiled biomass of thermotolerant oleaginous microalgae Acutodesmus dimorphus. *RSC Adv.* July 2016;6(76) [Google Scholar]

[18] Kokila T., Ramesh P.S., Geetha D. Biosynthesis of silver nanoparticles from Cavendish banana peel extract and its antibacterial and free radical scavenging assay: a novel biological approach. *Appl. Nanosci.* 2015;2015(5):911–920. [Google Scholar]

[19] Krishnaraj C., Jagan E.G., Rajasekar S., Selvakumar P., Kalaichelvan P.T. Synthesis of silver nanoparticles using Acalyphaindica leaf extracts and its antibacterial activity against water borne pathogens. *Colloids Surfaces B Biointerfaces.* 2010;76:50–56. [PubMed] [Google Scholar]
[20] Nagarajan A., Alderson P.G., Arivalagan U. Effective surface sterilization and callus induction protocol for copper leaf (Acalypha wilkesiana) *Int. J. Appl. Biotechnol. Biochem.* 2003;3(1):37–49. [Google Scholar]
[21] Olivier T., David S., Bertrand P., Erick D. The population genetics of commensal Escherichia coli. *Nat. Rev. Microbiol.* 2010;8(3):207–217. [PubMed] [Google Scholar]
[22] Oluwaniyi O.O., Adegoke H.I., Adesuji E.T., Alabi A.B., Bodede S.O., Labulo A.H., Oseghale C.O. Biosynthesis of silver nanoparticles using aqueous leaf extract of Thevetia peruviana Juss and its antimicrobial activities. *Appl. Nanosci.* 2016;6(6):903–912. [Google Scholar]
[23] Oyelani O.A., Onayemi O., Oladimeji F.A., Ogundani O.A., Olugbade T.A., Onawunmi G.O. Clinical evaluation of Acalypha ointment in the treatment of superficial fungal skin diseases. *Phytother Res.* 2003;17:555–557. [PubMed] [Google Scholar]
[24] Pochapski M.T., Fosquiera E.C., Esmerino L.A., dos Santos E.B., Farago P.V., Santos F.A., Groppo F.C. Phytochemical screening, antioxidant, and antimicrobial activities of the crude leaves' extract from *Ipomoea batatas* (L.) Lam. *Pharmacogn. Mag.* 2011;7(26):165–171. [PMC free article] [PubMed] [Google Scholar]
[25] Prathna T.C., Chandrasekaran N., Ashok M., Raichur A.M. Kinetic evolution studies of silver nanoparticles in a bio-based green synthesis process. *Colloid. Surf. Physicochem. Eng. Asp.* 2011;377:212–216. [Google Scholar]
[26] Ravindran A., Chandran P., Khan S.S. Biofunctionalized silver nanoparticles: advances and prospects. *Colloids Surfaces B Biointerfaces.* 2013;105:342–352. [PubMed] [Google Scholar]
[27] Rivera-Rangela R.D., González-Muñoza M.P., Avila-Rodrigueza M., Razo-Lazcanoa T.A., Solans Conxita. Green synthesis of silver nanoparticles in oil-in-water microemulsion and nano-emulsion using geranium leaf aqueous extract as a reducing agent. *Colloids Surf., A.* 2018;536:60–67. [Google Scholar]
[28] Senguttuvan J., Paulsamy S., Karthika K. Phytochemical analysis and evaluation of leaf and root parts of the medicinal herb, *Hypochaeris radicata L.* for *in vitro* antioxidant activities. *Asian Pac. J. Trop. Biomed.* 2014;4(Suppl 1):S359–S367. [PMC free article] [PubMed] [Google Scholar]
[29] Shankar S.S., Rai A., Ahmad A., Sastry M.J. Rapid synthesis of Au, Ag and bimetallic Au shell nanoparticles using Neem. *J. Colloid Interface Sci.* 2004;275:496–502. [PubMed] [Google Scholar]
[30] Shiv S.S., Absar A., Murali S. Geranium leaf assisted biosynthesis of silver nanoparticles. *Biotechnol. Prog.* 2003;19(6):1627–1631. [PubMed] [Google Scholar]
[31] Singh S., Saikia J.P., Buragohain A.K. A novel 'green' synthesis of colloidal silver nanoparticles (SNP) using Dillenia indica fruit extract. *Colloids Surfaces B Biointerfaces.* 2013;102:83–85. [PubMed] [Google Scholar]
[32] Tippayawat P., Phromviyo N., Boueroy P., Chompoosor A. Green synthesis of silver nanoparticles in aloe vera plant extract prepared by a hydrothermal method and their synergistic antibacterial activity. *PeerJ.* 2016;4 [PMC free article] [PubMed] [Google Scholar]
[33] Tong S.Y., Davis J.S., Eichenberger E., Holland T.L., Fowler V.G. Staphylococcus aureus infections: epidemiology, pathophysiology, clinical manifestations, and management. *Clin. Microbiol. Rev.* 2015;28(3):603–661. [PMC free article] [PubMed] [Google Scholar]
[34] Tran T.T.T., Vu T.H.T., Hanh Thi Nguyen T.H. Biosynthesis of silver nanoparticles using Tithonia diversifolia leaf extract and their antimicrobial activity. *Mater. Lett.* 2013;105:220–223. [Google Scholar]
[35] Udobang J.A., Nwafor P.A., Okokon J.E. Analgesic and antimalarial activities of crude leaf extract and fractions of *Acalypha wilkesiana. J. Ethnopharmacol.* 2010;127:373–378. [PubMed] [Google Scholar]
[36] Vijayaraghavan K., Kamala Nalini S.P., Prakash N.U., Madhankumar D. Biomimetic synthesis of silver nanoparticles by aqueous extract of *Syzygium aromaticum*. *Mater. Lett.* 2012;75:33–35. [Google Scholar]
[37] Wen C., Shao M., Zhuo S., Lin Z., Kang Z. Silver/graphene nanocomposite: thermal decom-10 position prep catalytic performance. *Mater. Chem. Phys.* 2012;135:780–785. [Google Scholar]
[38] Yong S.J., Kim S.K.B. Rapid biological synthesis of silver nanoparticles using plant leaf extracts. *Bioproc. Biosyst. Eng.* 2008;32(1):79–84. [PubMed] [Google Scholar]
[39] Zhang X.-F., Liu Z.-G., Shen W., Gurunathan S. Silver nanoparticles: synthesis, (2014) characterization, properties, applications, and therapeutic approaches. *Int. J. Mol. Sci.* 2016;17(9):1534. [PMC free article] [PubMed] [Google Scholar]